Surface morphology improvement by diethylzinc doping on metamorphic InAs on GaAs using MOVPE

メタデータ	言語: en
	出版者: Elsevier
	公開日: 2023-06-19
	キーワード (Ja):
	キーワード (En):
	作成者: 荒井, 昌和, Nakagawa, Shota, Hombu Koki, Hirata, Yasushi, 前田, 幸治
	メールアドレス:
	所属:
URL	http://hdl.handle.net/10458/0002000001

Journal of Crystal Growth 617 (2023) 127274

Contents lists available at ScienceDirect

Journal of Crystal Growth

journal homepage: www.elsevier.com/locate/jcrysgro

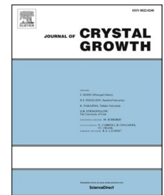

Surface morphology improvement by diethylzinc doping on metamorphic InAs on GaAs using MOVPE

Masakazu Arai *, Shota Nakagawa, Koki Hombu, Yasushi Hirata, Koji Maeda

Faculty of Engineering, University of Miyazaki, 1-1 Gakuen Kibanadai Nishi, Miyazaki 889-2192, Japan

ARTICLE INFO

Communicated by Elke Meissner

Keywords:
A3. Low press
Metalorganic vapor phase epitaxy
B2. Semiconducting III-V materials
A1. Doping
A1. Crystal morphology
A1. Atomic force microscopy
B3. Infrared devices

ABSTRACT

We investigate the effect of diethylzinc doping on surface roughness during InAs growth on a GaAs substrate using metal-organic vapor phase epitaxy. Surface roughness was measured using atomic force microscopy and scanning electron microscopy. The surface flatness was considerably improved following the introduction of diethylzinc. Furthermore, we evaluate the Raman scattering and X-ray diffraction to investigate the crystallinity. The results confirm that diethylzinc doping effectively improves surface roughness.

1. Introduction

Mid-infrared photonic devices, such as lasers [1–4] and photodiodes [5–6] are crucial for optical gas sensing and utilizing new wavelengths for fiber communication. These devices, except for quantum cascade lasers, use narrow-gap materials and are usually grown on GaSb or InAs substrates. However, these substrates are expensive and have inferior crystal quality compared with that of the widely used GaAs and InP substrates. Moreover, semi-insulating InAs and GaSb substrates are lacking. Therefore, metamorphic growth (heteroepitaxial growth) to fabricate a virtual InAs(Sb) substrate on GaAs or InP is a breakthrough growth technique to realize low-cost and high-quality mid-infrared photonic devices. In state-of-the-art reports of midinfrared detectors on GaAs substrate, the devices suffer from poor surface roughness [7–9]. Additionally, InAs has a high electron mobility. Therefore, metamorphic InAs growth is applicable to high-electron-mobility transistors [10–12] and heterojunction bipolar transistors [13–14]. The metamorphic growth is affected by the growth conditions and can be controlled by facet growth [15–16]. Several studies to improve the crystal quality of InAs, such as two-step growth [17], graded composition buffer [18], off-cut substrate [19], bismuth doping [20–21], and Te doping [22] have been reported. Additional doping materials used to change the surface reaction energy are called surfactants. Surfactants for other mother materials, such as silicon [23–25], GaAs [26], Cu [27], InGaAs [28–31], InAs dot [32–33], InAsSb [34], and AlGaInAs [35] have been reported. However, to the best of our knowledge, the effect of Zn doping on the surface roughness of InAs has not been fully investigated.

This study introduces diethylzinc (DEZn) doping into an InAs buffer and validates the improvement in the surface roughness of InAs. We examine the details of the growth conditions of metal–organic vapor phase epitaxy (MOVPE) and report the measured results. Compared with our previous study [36], several experimental data, such as Raman spectroscopy, are presented in this study to evaluate the crystallinity. Compared to the report on Zn-doped AlGaInAs [35], the doping concentration in this study is higher. Further, we examine the flow rate dependence of dopants in more detail.

2. Experimental methods

MOVPE is a commercially available vertical type, one wafer (3-inch) susceptor, a carbon heater, and a face-up type (SV3001, EpiQuest, Japan). The growth pressure was set to 10 kPa. The carrier gas was H_2 and metal–organic materials were supplied by H_2 bubbling. The H_2 carrier gas flow rate was set at 3000 sccm. The metal–organic materials used in these experiments were triethylgallium (TEGa) and trimethylindium (TMIn), as group III sources. Hydrogen-diluted (20%) arsine (AsH_3) gas was used as the group V source. The molar V/III ratio of InAs growth is 116. In general, surface migration is suppressed under a high

* Corresponding author.
E-mail address: arai.masakazu@cc.miyazaki-u.ac.jp (M. Arai).

https://doi.org/10.1016/j.jcrysgro.2023.127274
Received 2 February 2023; Received in revised form 22 April 2023; Accepted 17 May 2023
Available online 22 May 2023
0022-0248/© 2023 The Authors. Published by Elsevier B.V. This is an open access article under the CC BY-NC-ND license (http://creativecommons.org/licenses/by-nc-nd/4.0/).

V/III ratio. Moreover, the migration is suppressed under low temperature growth. Diethylzinc was used as the dopant source. A dilution line was used to widen the flow range of DEZn. Atomic force microscopy (AFM) (AFM5200S, Hitachi High-Tech, Japan) with a Si cantilever was used to evaluate the surface roughness. Scanning electron microscopy (SEM) (S-5500, Hitachi High-Tech, Japan) was used to perform surface and cross-sectional observations. The carrier concentration was measured using a Hall effect measurement system (HL5500PC, Bio-Rad, USA). The X-ray rocking curve was measured by using an X-ray diffraction (XRD) measurement system (X'Pert-Pro, PANalytical, England). Raman spectra were obtained at room temperature (approximately 23 °C) using a HORIBA Sci. LabRAM HR evolution system. The Nd: YAG 532 nm excitation laser was focused on the sample with an × 100 microscope objective and the power was maintained at 4 mW. The penetration depth of the excitation light was approximately 200 nm.

3. Results and discussion

In this section, we discuss the growth temperature dependence of the surface morphology of undoped InAs on GaAs substrates. The growth temperature of InAs was varied from 450 to 650 °C on a GaAs buffer grown at 650 °C. The thickness of InAs was 300 nm. The AFM image and bird-view SEM results of the growth at 500 and 600 °C are shown in Fig. 1. The measured area in the AFM images is 10 μm^2. The (1 1 1) facet can be clearly seen in the case of the growth at 600 °C. The growth temperature dependence of the root mean square (RMS) roughness measured using AFM is shown in Fig. 2. The surface morphology degraded beyond 550 °C. Growth temperatures below 500 °C resulted in carbon and oxygen incorporation. Therefore, we chose a growth temperature of 500 °C for InAs on the GaAs substrate. The RMS roughness of the undoped InAs is 12 μm. In this experiment, the low temperature growth and high V/III ratio are crucial for improving the surface roughness for initial thin film growth. Accordingly, we investigated the effect of doping on the growth of InAs to improve the surface roughness at 500 °C.

We investigated the DEZn flow-rate dependence of Zn-doped InAs. Once the GaAs buffer was grown on the GaAs substrate at 650 °C, a 300-nm-thick InAs was grown on the GaAs buffer at 500 °C with flowing DEZn. The DEZn flow-rate dependence of the RMS value of the surface

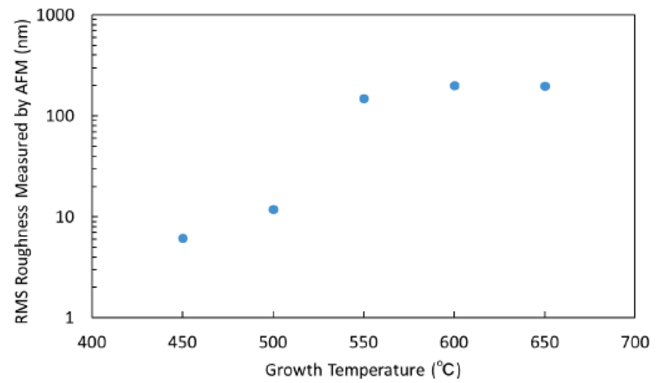

Fig. 2. Growth temperature dependence of the RMS roughness measured using AFM.

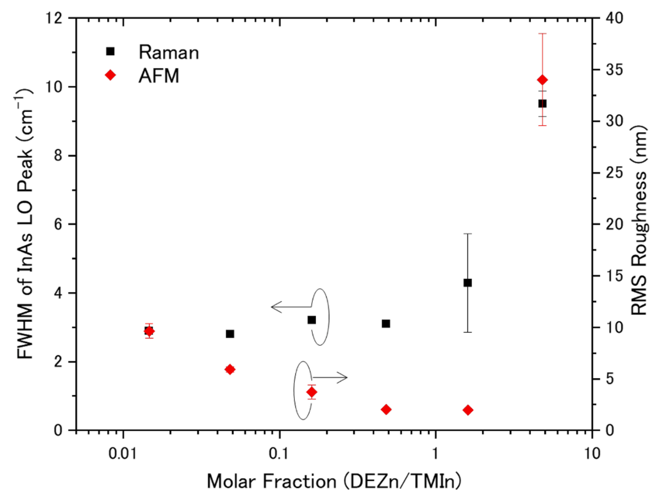

Fig. 3. DEZn flow-rate dependence of the surface roughness of the InAs layer on GaAs substrates.

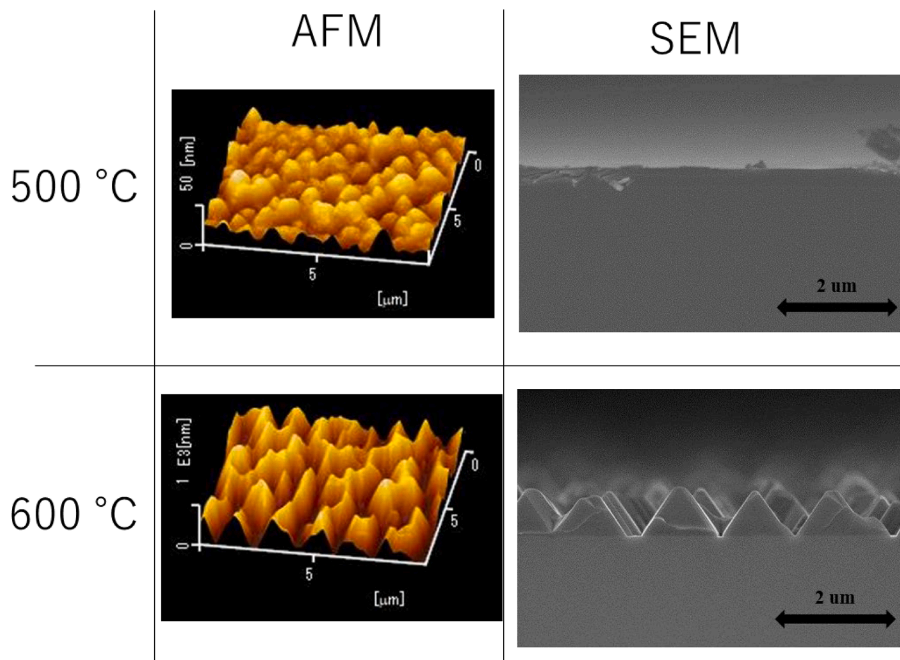

Fig. 1. Results of AFM and cross-sectional SEM images of the samples grown at 500 and 600 °C.

roughness measured using AFM is shown in Fig. 3 (Axis: left-hand side). The flow rate of DEZn was changed from 0.16 to 50 sccm, which corresponds to a molar fraction (DEZn/TMIn) of 0.015 to 4.8. The carrier concentrations measured by the Hall Effect measurement of the minimum and maximum molar fractions are 9×10^{18} and 4×10^{19} (cm^{-3}), respectively. Since the flow rates are extremely high, the carrier concentration was saturated. The DEZn flow rate in this experiment is significantly higher than that reported for Zn-InAlGaAs [35]. The surface roughness improved with an increase in the DEZn molar fraction flow up to 1.6. However, it deteriorated significantly when the mole fraction reached 4.8.

Subsequently, the initial stage of the InAs growth mode was observed. The growth temperature was fixed at 500 °C and the molar fraction of DEZn was fixed at 1.6., which is the best flatness, as illustrated in Fig. 3. We prepared four variations of undoped InAs with thicknesses of 2, 10, 50, and 300 nm by adjusting the growth time. The corresponding Zn-doped InAs thicknesses for the same growth time are 1.6, 8.1, 40.5, and 241 nm, respectively, primarily because of the reduced growth rate owing to the addition of DEZn. A similar tendency was reported in case of the InAlGaAs layer in [37].

The thickness dependence of the surface roughness with and without DEZn doping measured by AFM is shown in Fig. 4. With an increasing InAs thickness, up to approximately 50 nm, the surface roughness increases monotonically. In this region, the islands are coalesced and enlarged. Subsequently, the overgrown layer fills the gaps among the islands, gradually improving the flatness. When the thickness of the Zn-InAs film is 241 nm, the surface of the Zn-doped InAs is much flatter than that of the undoped 300-nm-thick InAs. We investigated the reason for such a large difference. There are few reports of surface flatness improvement at thick growth under low temperature and high V/III ratio growth. However, the opposite effect was reported in [39]. In this study, the low temperature and low V/III ratio growth were used for InAs growth on a GaAs substrate. In comparing the 25 nm and 360 nm thick InAs layers, the surface roughness was deteriorated in the thicker layer. The deterioration can be attributed to the ridge formation caused by anisotropic surface migration reflected by the chemical kinetics. Moreover, the misoriented substrate suppresses the ridge formation due to the reduced surface migration affected by the increased terrace and edge. In our experiment, a low temperature and a high V/III ratio of over 100 were maintained. Therefore, the ridge formation of thick layer growth could be suppressed. Additionally, in [40], the diffusive Be doped InGaAs on GaAs exhibits the better surface flatness than undoped layer. This was explained by the reconstruction in grown layer by enhancing the dopant diffusion. We believe that the sudden improvement in the case of 300-nm-thick Zn-InAs can be attributed to a similar effect caused by zinc diffusion.

A comparison of the initial nucleation between undoped and Zn-doped InAs on GaAs is shown in Fig. 5. The growth time corresponds to a 2-nm thick (Zn-doped 1.6-nm thick) film. The surface coverage area ratio of the undoped InAs on the GaAs surface is 37%. Meanwhile, the ratio of Zn-doped InAs is 43%. The coverage ratio of InAs on GaAs increases with the introduction of DEZn flow. This can be attributed to the shortened migration length caused by the introduction of the DEZn flow.

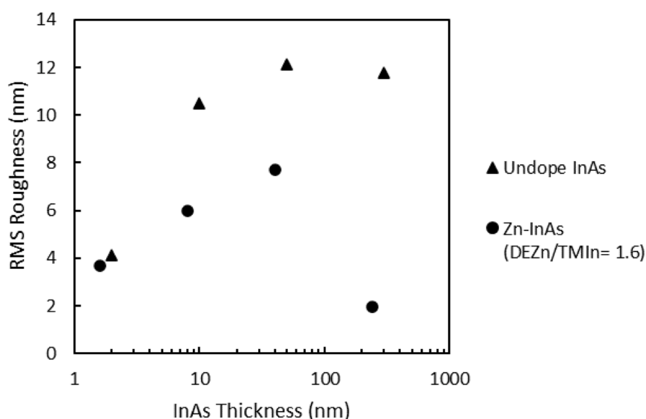

Fig. 4. Thickness dependence of the RMS roughness in comparison between undoped and Zn-doped InAs on GaAs substrates.

Raman scattering spectra of the Zn-doped InAs layer fitted with Lorenz functions are shown in Fig. 6. The highest peak at 238 cm^{-1} is attributed to the LO-phonon mode. The broad peak at 218 cm^{-1} is attributed to the forbidden TO-phonon mode. The peak at 230 cm^{-1} may be attributed to the LO-phonon-plasmon-coupled (LOPC) mode [38].

The thickness dependence of the full width at half maximum (FWHM) of the LO peak is shown in Fig. 7. The FWHM between the 300-nm thick undoped InAs and 241-nm-thick Zn-InAs is almost the same. Therefore, the crystallinity of both samples is the same. In addition, we measured the X-ray rocking curve on both 300-nm-thick i-InAs and 241-nm-thick Zn-InAs layer shown in Fig. 7. Both samples exhibit a single peak, which is the same as the 500 °C sample of Khanderkar's report [19]. The FWHM of the rocking curve of undoped InAs and Zn-doped InAs are 928 and 1390 arcseconds, respectively. However, the Zn-InAs film is thinner than i-InAs because of the growth rate change induced by Zn doping. This thickness difference also affects the FWHM. The thinner layer exhibits a wider FWHM. Therefore, we believe that the crystallinity between undoped and Zn-doped InAs on GaAs is almost the same. This is consistent with the results obtained by the Raman scattering measurement mentioned in the next section. Furthermore, these results correspond to the threading dislocation density in the cross-sectional transmission electron microscope (TEM) image. Both samples have the same order of magnitude 10^9 (cm^{-2}) on the threading dislocation density.

The DEZn molar fraction dependence of the FWHM of LO peaks by Raman scattering is shown in Fig. 3 (Axis: left-hand side). In the DEZn molar fraction range from 0.015 to 0.48, the FWHM of the LO peak is almost the same. Only the error bars of 1.6 in the DEZn molar fraction are large because of the significant dependence on the measurement location. When the DEZn molar fraction increases to 4.8, the LO peak broadens and the surface roughness suddenly deteriorates. This tendency is almost the same between the width of the LO peak and the RMS value.

4. Conclusions

We investigated the growth temperature dependence on the surface roughness of an undoped InAs layer on a GaAs substrate and validated that low-temperature growth below 550 °C effectively suppresses facet formation. Moreover, we evaluated the effect of highly concentrated DEZn doping on the surface roughness during InAs growth and validated that the introduction of DEZn significantly improves the surface flatness. The RMS roughness (10 μm^2) measured using AFM was as low as 2 nm. The LO peak width measured using Raman spectroscopy and the surface flatness measured using AFM had some correlations. Therefore, DEZn doping effectively improved the surface roughness without deteriorating the crystallinity. This technique can effectively improve the surface roughness of a device on a p-type-substrate. Importantly, the Zn-diffusion should be controlled carefully. To further improve the crystallinity, a combination of the annealing treatment and two-step growth would be effective. This technique will render the production of low-cost, high-quality, mid-infrared photonic devices feasible.

Declaration of Competing Interest

The authors declare that they have no known competing financial interests or personal relationships that could have appeared to influence the work reported in this paper.

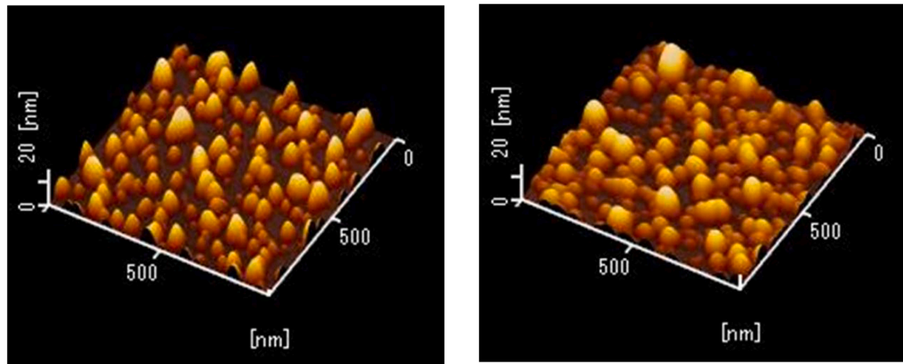

Fig. 5. Comparison of the AFM image of the initial stage of InAs growth (a) undoped (b) Zn-doped samples.

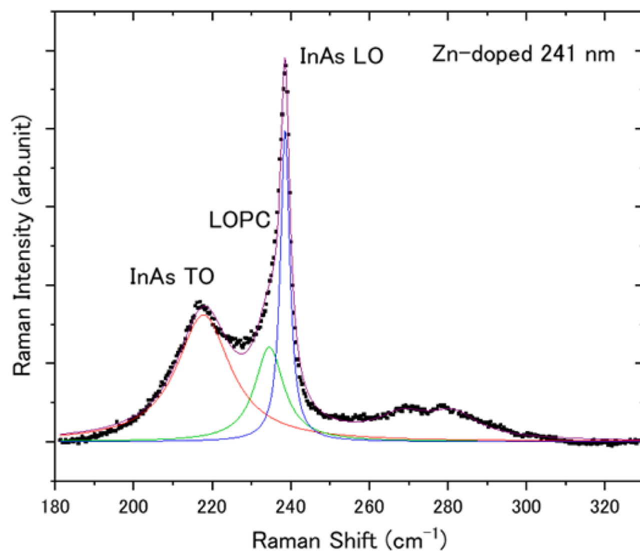

Fig. 6. Measured Raman spectrum of the 241-nm-thick Zn-doped InAs.

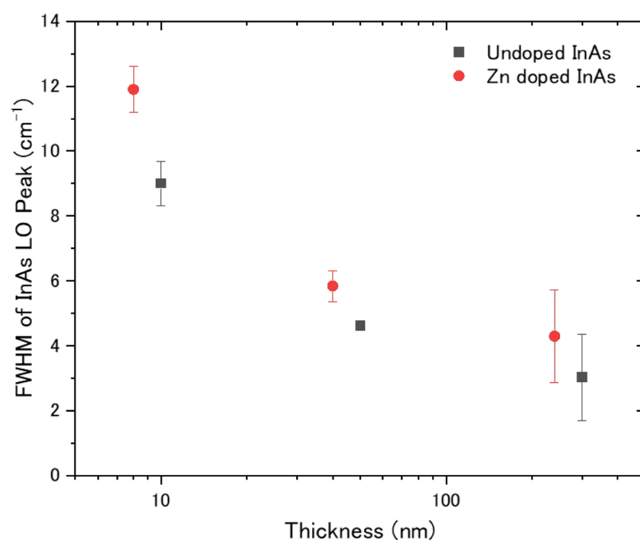

Fig. 7. Layer thickness dependence of the FWHM of LO peaks.

Data availability

The authors do not have permission to share data.

Acknowledgment

This study was supported by JSPS KAKENHI (grant number JP19K04515).

References

[1] R.M. Biefeld, A.A. Allerman, S.R. Kurtz, J.H. Burkhart, J. Electron. Mater. 26 (1997) 1225.
[2] C.A. Wang, H.K. Choi, J. Electron. Mater. 26 (1997) 1231.
[3] G. Belenky, L. Shterengas, G. Kipshidze, T. Hosoda, Ieee,, J. Sel. Top. Quantum Electron. 17 (2011) 1426.
[4] G.K. Veerabathran, S. Sprengel, A. Andrejew, M.-C. Amann, 110, 071104 (2017).
[5] A.P. Craig, A.R.J. Marshall, Z.-B. Tian, S. Krishna, A. Krier, Appl. Phys. Lett. 103 (2013), 253502.
[6] D.H. Wu, A. Dehzangi, Y.Y. Zhang, M. Razeghi, Appl. Phys. Lett. 112 (2018), 241103.
[7] D.C.M. Kwan, M. Kesaria, J.J. Jimenez, V. Srivastava, M. Delmas, B.L. Liang, F. M. Morales, D.L. Huffaker, Nat. Sci. Reports 12 (2022) 11616.
[8] P. Martyniuk, D. Benyahia, Opto-Electron. Rev. 31 (2023) e144557.
[9] S. Woo, E. Yeon, R.J. Chu, J. Kyhm, H. Son, H.W. Jang, D. Jung, W.J. Choi, Appl. Surface Sci. 623 (2023), 156899.
[10] H. Masato, T. Matsuno, K. Inoue, Jpn. J. Appl. Phys. 30 (1991) 3850.
[11] T. Mishima, K. Higuchi, M. Mori, M. Kudo, J. Cryst. Growth 150 (1995) 1230.
[12] K.C. Hwang, P.C. Chao, C. Creamer, K.B. Nichols, S. Wang, D. Tu, W. Kong, D. Dugas, G. Patton, IEEE Electron Dev. Lett. 20 (1999) 551.
[13] H.Q. Zheng, K. Radhakrishnan, H. Wang, K.H. Yuan, S.F. Yoon, G.I. Ng, Appl. Phys. Lett. 77 (2000) 869.
[14] W.K. Liu, D. Lubyshev, Y. Wu, X.M. Fang, T. Yurasits, A.B. Cornfeld, D. Mensa, S. Jaganathan, R. Pullela, M. Dahlstrom, P.K. Sundrarajan, T. Mathew, and M. Rodwell, in: Proceedings of the 13th International Conference on InP and Related Materials 284 (2001).
[15] B. Kunert, R. Alcotte, Y. Mols, M. Baryshnikova, N. Waldron, N. Collaert, R. Langer, Cryst. Growth Des. 21 (2021) 1657.
[16] J.S. Mangum, S. Theingi, M.A. Seteiner, W.E. McMahon, E.L. Warren, Crytal. Growth Des. 21 (2021) 5955.
[17] H. Yuan, S.J. Chua, Z. Miao, J. Dong, Y. Wang, Int. J. Cryst. Growth 273 (2004) 63.
[18] Y. Jeong, H. Choi, T. Suzuki, J. Cryst. Growth 301–302 (2007) 235.
[19] A.A. Khandekar, G. Suryanarayanan, S.E. Babcock, T.F. Kuech, J. Cryst. Growth 292 (2006) 40.
[20] N. Grandjean, J. Massies, V.H. Etgens, Phys. Rev. Lett. 69 (1992) 796.
[21] H. Zhao, A. Malko, Z.H. Lai, J. Crys. Growth 425 (2015) 89.
[22] P.h. Komninou, P. Gladkov, T.h. Karakostas, J. Pangrác, O. Pacherová, J. Vaniš, E. Hulicius, J. Cryst. Growth 396 (2014) 54.
[23] R.M. Tromp, M.C. Reuter, Phys. Rev. Lett. 68 (1992) 954.
[24] S. Iwanari, K. Takayanagi, J. Cryst. Growth 119 (1992) 229.
[25] S. Iwanari, Y. Kimura, K. Takayanagi, J. Cryst. Growth 119 (1992) 241.
[26] J. Massies, N. Grandjean, Phys. Rev. B 48 (11) (1993) 8502.
[27] J. Camarero, J. Ferrón, V. Cros, L. Gómez, A.L. Vázquez de Parga, J.M. Gallego, J. E. Prieto, J.J. de Miguel, R. Miranda, Phys. Rev. Lett. 81 (1998) 850.
[28] J.C. Harmand, L.H. Li, G. Patriarche, L. Travers, Appl. Phys. Lett. 84 (2004) 3981.
[29] T. Sato, M. Mitsuhara, T. Watanabe, Y. Kondo, Appl. Phys. Lett. 87 (2005), 211903.
[30] T. Sato, M. Mitsuhara, T. Watanabe, K. Kasaya, T. Takeshita, Y. Kondo, IEEE J. Sel. Top. Quantum Electron. 13 (2005) 1079.
[31] T. Sato, Y. Kondo, T. Sekiguchi, T. Suemasu, Appl. Phys. Express 1 (2008), 111202.

[32] B.N. Zvonkov, I.A. Karpovich, N.V. Baidus, D.O. Filatov, S.V. Morozov, Y. Y. Gushina, Nanotechnology 11 (2000) 221.
[33] D.V. Forbes, C.G. Bailery, S. Polly, S.M. Hubbard, W. Maurer, and R.P. Raffaelle, in: Proc. of 34th IEEE Photovoltaic Specialists Conference, 2009.
[34] J.G. Cederberg, R.M. Biefeld, Proc. of Mater. Res. Soc. Symp. 749. W2.6 (2003).
[35] L. Zhang, Z. Chen, X. Liu, S. Huang, Z. Fei, J. Li, G. Wang, Jpn. J. Appl. Phys. 59 (2020), 025507.
[36] S. Nakagawa, Y. Imamura, Y. Hirata, K. Maeda, M. Arai, Microoptics Conf. MOC2021 (2021) PO-52.
[37] H. Yokoyama, T. Hoshi, N. Shigekawa, M. Ida, Jpn. J. Appl. Phys. 51 (2012), 025601.
[38] H.Y. Deng, J.H. Guo, Y. Zhang, R. Cong, G.J. Hu, G.L. Yu, N. Dai, Appl. Surf. Sci. 288 (2014) 40.
[39] H.B. Naceur, I. Moussa, O. Tottereau, A. Rebey, B. El Jani, Physica E 41 (2009) 1779.
[40] I. Tångring, Y. X. Song, Z.H. Lai, S.M. Wang, M. Sadeghi, A. Larsson, J. Cryst. Growth 311 (2009) 1684.